

THE EFFECT OF BUILD ORIENTATION ON THE MECHANICAL PROPERTIES IN INKJET 3D PRINTING

J. Mueller*, K. Shea*

*Engineering Design and Computing Laboratory, Department of Mechanical and Process Engineering, ETH Zurich, 8092 Zurich, Switzerland

REVIEWED

Abstract

It is known that part orientation plays an important role in 3D printing and especially in inkjet 3D printing, where the layers are more distinct than in other processes. Despite many investigations in this direction, previous research focused mainly on build orientations along the three main axes X, Y and Z. For advanced purposes such as optimization, however, it is important to know what happens in combined alignments between the main axes. The authors hypothesize and show that the transition is not linear and that, despite prior studies, the weakest properties are not found when the parts are aligned along the Z direction. The discovered effects can partially be attributed to shear forces in the material, which act between the layers when the parts are not aligned orthogonally to the main axes. To accurately characterize the three-dimensional space, the mixture design method has successfully been introduced to the area of 3D printing and proven to be an efficient tool that can also be used for other processes. With the results of this study, designers and engineers are now able to analyze and predict part properties on a much higher level than before.

1. Introduction

Among the different factors affecting the mechanical properties of fabricated parts, the build orientation is often one of the most influential ones and one of the few factors prevalent in almost all additive manufacturing (AM) processes [1, 2]. The build orientation impacts the accuracy, build time, cost, surface roughness and much more, and its optimization is a fundamental problem in AM which has been tackled by many researchers [3, 4], also from the theoretical side [1, 5, 6]. In many aspects, the effect on the mechanical properties is the most important one as it determines the functionality and not just the visual aspects of a part [7], yet no commercially available software allows for positioning parts on the print table according to the load introduction and direction. One possible reason is that most processes and their effects still aren't fully understood. In order to get a better understanding, empirical data need to be collected through experiments, which can then be used in models. Extensive research has been undertaken in the area [3, 5, 8], but most of it focused on either orientations along the main axes of the coordinate system, or on continuous orientations within only one plane instead of considering the full three-dimensional space. While in some processes, such as in Fused Deposition Modeling (FDM), the effect of the orientation is relatively small because of indistinct layers [8–10], in other processes such as in inkjet 3D printing, the effect cannot be neglected [11–14]. This is especially true for functional structures such as lattices, where the local load directions of the struts are

spatial, even if the global load direction is parallel to a main axis. In order for such structures to perform, they need to be designed and often optimized [15, 16], which is only possible when accurate material data is available. Gathering accurate material data for all possible build orientations, however, can be costly. A trade-off needs to be found for the required accuracy and the experimental cost. Hence, the mixture design, a statistical tool commonly used in chemistry, will be adapted and introduced into the field. It is tested for its applicability and robustness before conducting the main tests for the most common load cases compression and tension. The work is based on the inkjet 3D printing process, and the trends of the results and models are valid also for similar processes.

In the background section we discuss the relevant literature and put it into perspective with other AM processes. We then describe the materials and methods, and present the results in section four. A discussion of the results is provided and conclusions are drawn in the last section of the report.

2. Background

Additive manufacturing or 3D printing is defined as a layer based manufacturing process [17]. This statement generally holds true, but, due to the large amount of different printing processes, sometimes the layers are not very distinct. For example, in Selective Laser Sintering (SLS) and Fused Deposition Modelling (FDM), the material is cured voxel by voxel, and not line by line or layer by layer. Hence, the bonding strength between two layers is identical to the bonding between two printed lines within a layer, with only a difference in time. Looking at the global properties, the printing or curing path can be designed such that almost isotropic parts are created. Isotropy, however, is not always the goal as there is often only one load direction required for which the mechanical properties can be optimized. In those cases, the anisotropy is enforced. Less freedom is available in inkjet 3D printing, where the variances in terms of the mechanical properties sometimes reach 30%, which has been investigated on different printer types: Objet30 [19], Objet Eden 260 [18] and Objet Eden 330 [20–22]. The Objet350 Connex, which was investigated by Barclift and Williams [11], is closest to the printer used in this work, the Stratasys Objet500 Connex3. On the Connex3, the effect of the build orientation on the mechanical properties was investigated by Mueller et al. [13, 14]. However, all of these investigations have in common that they only look at build orientations along the three main axes. In this paper, the transition between the main axes is investigated for all possible build orientations. Since the Connex3 is one of the most advanced commercially available multi material printers [23], it can be considered to be representative for the current state-of-the-art in commercial inkjet 3D printing.

In comparison to inkjet 3D printing, the variations in FDM can range from about 9% in the strength [9], over 11% in both modulus and strength [8] to 28% in strength [10]. The large differences can mostly be attributed to the different print settings. For SLS, variations ranging from 7% to 47% are reported [24]. Note that in both of these processes the anisotropy is intended and can be drastically reduced by optimized alignment of the print or cure path, which is not the case in commercial inkjet 3D printing. In inkjet 3D printing, a print head with multiple, linearly aligned nozzles moves back and forth positioning the liquid material before curing it almost homogeneously through the attached ultra-violet (UV) lights. Hence, the layer itself is built in a

much shorter time compared to other processes. This yields a smaller anisotropy within the layer, but a larger one between the layers [13, 14], creating a structure with transversally isotropic properties. Roughly speaking it can be said that the smaller the ratio

$$v_f = \frac{\text{time to print one layer}}{\text{time to shift between layers}}$$

the higher the minimum anisotropy. This, however, cannot be generalized and needs to be investigated in detail for each individual process. v_f is also an indicator for a number of other effects, such as the printing time [25–28]. For a process with a small v_f , such as the inkjet 3D printing process, the print time drastically increases when the build orientation changes, whereas the change is much smaller for processes with a high v_f , like FDM [29, 30]. Since the build orientation is one of the early steps in the AM cycle, it has additional importance since it subsequently influences many following steps such as the slicing, support generation, tool path definition, fabrication, part removal and cleaning [7].

3. Materials and Methods

The experimental procedure is described based on the experimental design, printing and testing.

3.1 Experimental design

A response surface is applied to multiple measurement points which are analyzed experimentally. More specifically, an unaugmented mixture design [31] with three components is chosen that allows to define the proportions of the coordinate system, i.e. the X, Y and Z axes, as contributions to a blend. The axes are defined as components or factors of the design, as shown in Figure 1. The dots are the levels or settings of the factors. Then, a detailed in-plane measurement is conducted for the tension's Young's modulus in the XZ plane to investigate the suitability of the chosen experimental design and its settings, indicated in blue. Angles ranging from 0° to 90° are measured in 10° steps on 5 specimens for each point and compared to second and third polynomial degree models, which represent the simplex centroid (left) and simplex lattice degree 3 (right) models. The results are analyzed to find the best trade-off between accuracy and experimental cost, and the more suitable design is chosen for the main tests accordingly.

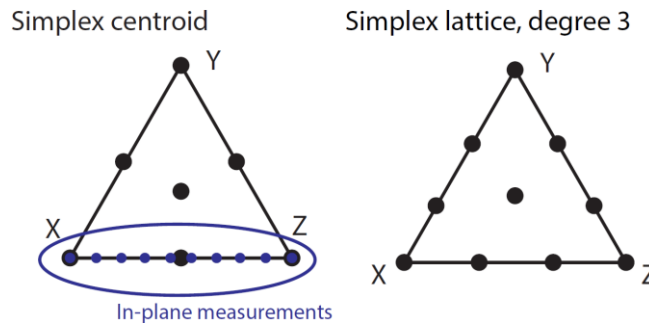


Figure 1: Unaugmented mixture designs. The black dots indicate the set measurements in relation to the axes and the blue dots indicate the in-plane measurements of the XZ plane.

3.2. Printing

All test-specimens are printed on a Stratasys Objet500 Connex3 printer under air-conditioned temperatures. Each test run is printed in a separate tray and the print head is cleaned before each run to prevent an influence through blocked nozzles [13, 14]. VeroWhitePlus (RGD835) model material from one batch is used in combination with SUP705 support material. To ensure a uniform surface finish and to prevent over-curing [19], the printers' mat option is used, with which the printer covers all surfaces in support material rather than adding it exclusively to overhanging features. Due to the slenderness, the specimens parallel to the Z axis are printed in an additional support structure made from model material. All parts are cleaned of support material with a Krumm RK 5 XL VA water-jet.

3.3. Mechanical testing

The tests are conducted on an Instron ElectroPuls E3000 universal testing machine. For the compression tests, the settings were chosen according to the ASTM D695-10 [32], i.e. the standard test specimen in the shape of a right cylinder with 'preferred dimensions' of 12.7 mm by 12.7 mm by 25.4 mm and a standard speed of testing of 1.3 mm/min. For the tensile properties, the ASTM D638-10 [33] standard is used. In order to fit the vertical build orientation on the tray, specimen geometry of type IV is chosen in combination with a constant testing speed of 50 mm/min. At least five replicates were tested for each setting and shuffled in print and test order to minimize random effects. As part of the mixture design, an Analysis of Variance (ANOVA) is conducted for each test, which provides information on the statistical significance of the results of different comparison groups. A critical p-value of $p_{crit}=0.05$ is chosen, indicating that effects with $p < 5\%$ are significant.

4. Results

Following, the empirical results of the tests are presented, starting with the in-plane tests. Then, the results of the mixture design tests are presented, followed by the application of the regression model, which yields the response surfaces.

4.1. In-plane tests

The results of the in-plane measurements of the XZ plane are shown for Young's modulus in Figure 2 with a black line. Curves for the simplex centroid and simplex lattice designs are added in red and green, respectively. Both curves are fitted to the measurement data in the start and end points, and at 45° for the centroid and at 30° and 60° for the simplex lattice. In blue, a linear interpolation between the start and end points is shown. All lines start at 2712 MPa. Between 0° and 45°, the interpolated measurement curve is well approximated by the simplex centroid and more so by simplex lattice, and all of those curves meet at 45° at about 2500 MPa. While the measurement and simplex lattice curves then further drop until they reach about 2472 MPa, the approximate minimum is reached at 45° for the simplex centroid. In this second half of the graph, the simplex lattice better approximates the measurements and at 90° all curves meet at 2600 MPa.

4.2. Mixture design tests

Compression. A summary of the compression test results shown in Table 1 and the final results of the mixture design, after applying the regression model, are shown in Figures 3a and 3c. The shapes of the fitted curves are similar for both mechanical properties and the build orientation along Y is the strongest with $E = 2396$ MPa and $US = 87$ MPa. Among the main axes, the lowest values are $E_{c,x} = 2272$ MPa and $US_{c,z} = 85$ MPa, with the remaining values laying in between at $E_{c,z} = 2358$ MPa and $US_{c,x} = 86$ MPa. The indices c and t stand for compression and tension, respectively, and are followed by the build orientation.

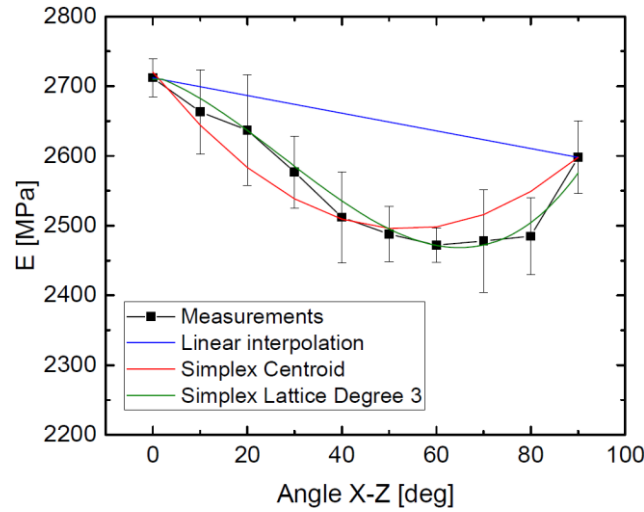


Figure 2: In-plane measurements (XZ) compared to linear and polynomial interpolations.

The properties in between two axes are always weaker than in the main directions and reach their minimum at approximately half way at 45° : $E_{c,xy} = 2177.63$ MPa, $US_{c,xy} = 84$ MPa, $E_{c,xz} = 2209$ MPa, $US_{c,xz} = 84$ MPa, $E_{c,yz} = 2171$ MPa and $US_{c,yz} = 85$ MPa. The weakest properties are found in between the three axes, close to the $0.5x + 0.5y + 0.5z$ orientation ($E_{c,xyz} = 2135$ MPa, $US_{c,xyz} = 84$ MPa).

Tension. The tension test results are shown in Table 2. The final tension test results after applying the regression model are shown in Figures 3b and 3d. For the Young's modulus, the shape is similar to the compression results: The peaks are at the main axes with lower values laying in between.

The values at X and Y are about the same ($E_{t,x} = 2765$ MPa, $E_{t,y} = 2778$ MPa), with the Z axis being considerably below ($E_{t,z} = 2689$ MPa). The intermediate values are always lower and reach their minima at about half way ($E_{t,xy} = 2684$ MPa, $E_{t,xz} = 2530$ MPa, $E_{t,yz} = 2579$ MPa). The lowest value found is, again, near the center at $0.5x + 0.5y + 0.5z$ ($E_{t,xyz} = 2539$ MPa). For the ultimate strength, the difference between the X and Y axes is marginal ($US_{t,x} = 62$ MPa, $US_{t,y} = 66$ MPa, $US_{t,xy} = 64$ MPa). This is true for all levels of Z, which has the lowest value at its main direction ($US_{t,z} = 41$ MPa). As opposed to the compression results, the intermediate values between the X and Z, and Y and Z axes show a convex trend ($US_{t,xz} = 57$ MPa, $US_{t,yz} = 58$ MPa).

Table 1: Compression test results for different print orientations. The numbers in the bracelets depict the standard deviation.

X	Y	Z	E [MPa]	UTS [MPa]
0	0	1	2351 (151)	85.12 (1.02)
0	1/2	1/2	2200 (196)	84.99 (0.53)
0	1	0	2389 (249)	87.40 (0.80)
1/3	1/3	1/3	2070 (120)	83.18 (0.78)
1/2	0	1/2	2237 (227)	84.14 (0.73)
1/2	1/2	0	2206 (212)	84.09 (0.62)
1	0	0	2265 (180)	86.10 (0.89)

Table 2: Tension test results for different print orientations. The numbers in the bracelets depict the standard deviation.

X	Y	Z	E [MPa]	US [MPa]
0	0	1	2687 (94)	41.01 (4.01)
0	1/2	1/2	2587 (104)	57.91 (3.50)
0	1	0	2776 (142)	66.08 (6.60)
1/3	1/3	1/3	2533 (70)	59.74 (2.10)
1/2	0	1/2	2537 (46)	57.56 (4.46)
1/2	1/2	0	2692 (48)	63.97 (5.91)
1	0	0	2763 (161)	62.19 (7.89)

In comparison, the Young's modulus of the compression tests is about 400 MPa (17%) higher than the one of the tension tests. For the ultimate strength, the tension tests provide about 21 MPa (32%) higher maximum values, but the difference increases for the intermediate values, especially when looking at the difference between the minimum values (43 MPa, 105%), or when closing in on Z. In terms of the variance, i.e. the difference between the maximum and minimum values, the compression provides, in average, considerably lower values ($\Delta E_c = 261$ MPa (12%), $\Delta E_t = 252$ MPa (10%), $\Delta US_c = 4$ MPa (5%), and $\Delta US_t = 25$ MPa (61%)).

Statistical significance. Part of the mixture design is an ANOVA, which provides information on the statistical relevance of the tests in terms of a p-value. The results for the tests and source terms are shown in Table 3. Since the linear terms are included in the quadratic terms, the quadratic terms are always of higher relevance. This is the case for the p-Values of E_c : With $p=0.396$, the linear term is far above the critical value $p_{crit}=0.05$. However, the quadratic terms ($p=0.008$) show that there exists a strong significance. This is especially true for the $X*Y$ ($p=0.041$) and $Y*Z$ combination ($p=0.008$). The notation $X*Y$ indicates interaction effects between the named factors. The value for $X*Z$ ($p=0.160$) is slightly above the critical value, but looking at the graph (Figure 3a) confirms the likelihood that the effect is also significant. For US_c , all p-values are <0.001 and thus highly statistically significant.

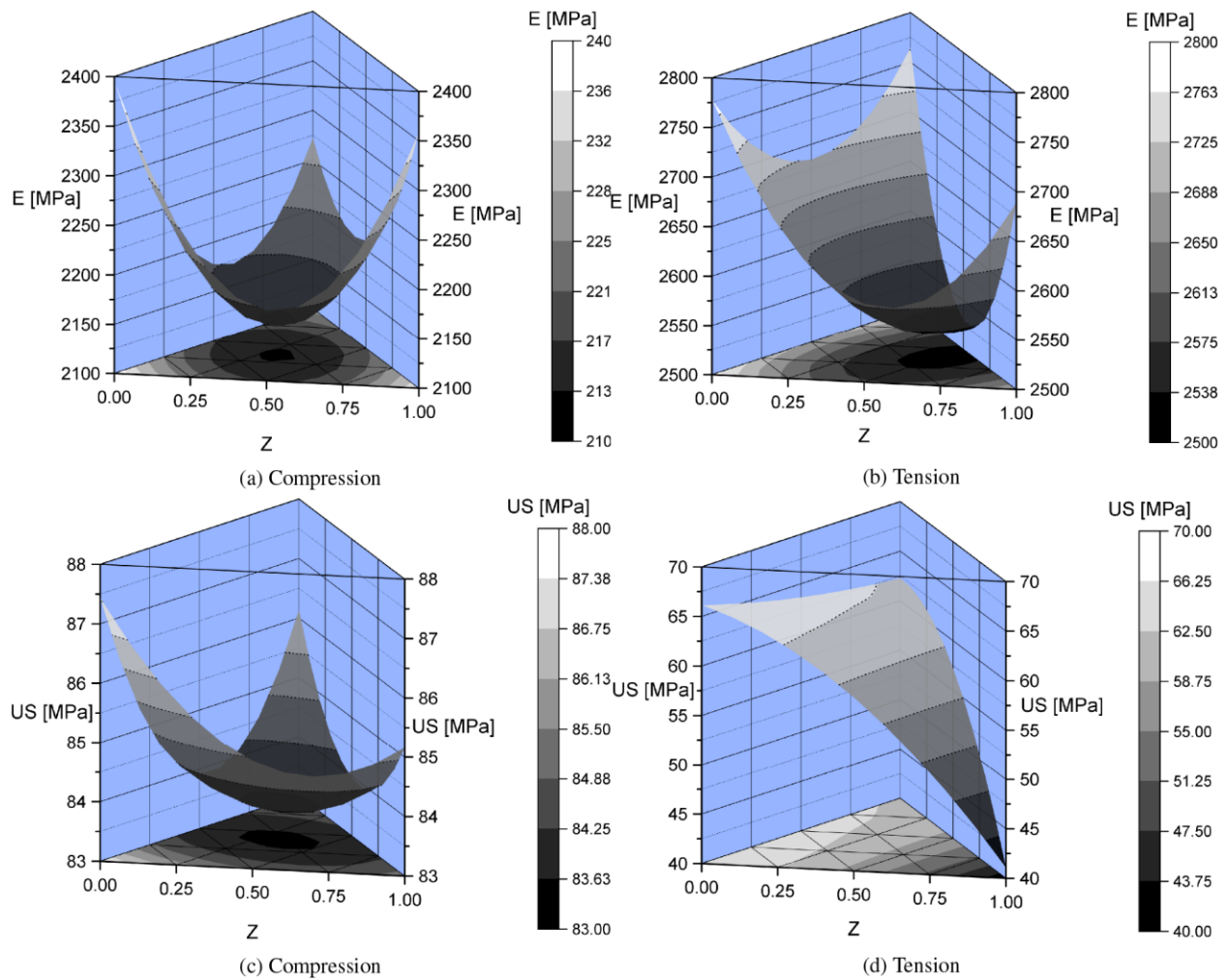


Figure 3: Compression and tension test results.

Table 3: Resulting p-values from the ANOVA.

Source	p			
	E_c	US_c	E_t	US_t
Linear	0.396	<0.001	0.298	<0.001
Quadratic	0.008	<0.001	<0.001	0.097
X*Y	0.041	<0.001	0.087	0.824
X*Z	0.160	<0.001	<0.001	0.039
Y*Z	0.008	<0.001	0.004	0.133

For E_t the situation is similar to E_c : A relatively high linear p-value (0.298) and high significances for the quadratic terms ($p < 0.001$). While the $X*Z$ ($p < 0.001$) and $Y*Z$ ($p = 0.004$) terms show a clear significance, the $X*Y$ interaction is slightly above the critical value ($p = 0.087$) and indeed, looking into the graph (Figure 3b) confirms that the significance is smaller compared to the others. For US_t , the linear terms show a strong significance ($p < 0.001$), and the overall quadratic terms are slightly above the threshold ($p = 0.097$). The $X*Y$ term does not show a significance, which is in agreement with its graph (Figure 3d). The $X*Z$ and $Y*Z$ significances ($p = 0.039$ and $p = 0.133$) are, however, close to the threshold and the graph shows indeed a strong decline towards Z.

5. Discussion

First, the design model decision is established based on the in-plane tests. Then, the main mixture design results tests are discussed and put into relation with a traditional process, injection molding.

5.1. In-plane tests

Although previous research did not specifically interpolate between the measurements, it is assumed that the whole width of the anisotropy is covered by inspecting build orientations only along the main axes. It is recognized that this approach is not sufficient when looking at the results of the mixture designs, but even more so when looking at the detailed in-plane measurements which are also compared to the linear interpolation (Figure 2). In contrast, an additional interpolation point in combination with a polynomial fit (degree 2), similar to the mixture design approach, drastically reduces the deviation error. Two additional points (polynomial degree 3) further increase the fitted accuracy, but add at least three measurement points per replication (Figure 1) or, in other words, 43% experimental cost. For this reason and due to the large number of tests conducted in this work, it has been decided to proceed with the simplex centroid design.

5.2. Mixture design tests

The effect of the layers in inkjet 3D printing can be described, in a simplified way, as polymer sheets, i.e. laminae, glued on top of each other to build adhesive joints. This is due to the fact that the liquid material is cured layer-wise, hence the intralaminar bonds are stronger than the interlaminar bonds. A similar phenomenon in composite materials is termed *shear extension coupling*: For out-of-plane alignments, i.e. when the normal stresses are not aligned with the printer's axes, the normal stresses cause shear strains and shear stresses cause extensional strains [34].

Compression. In in-plane loads, i.e. along X and Y, and in loads orthogonal to the plane, i.e. along Z, the loads are not straining the bonds directly. For the angles in between, shear forces are created which reach their maximum at about 45°, an effect also seen in the experimental results. As these forces directly affect the bonds, the mechanical properties are decreased (Figures 3a, 3c).

Tension. The same is valid for the tension, with the difference that in the Z orientation, the load also attacks the bonds between the layers. For the stiffness, the effect is visible, but weak, which is probably due to the fact that, as long as the bond lasts, the stiffness is not affected. The strength, however, is drastically reduced towards Z. This goes along with the recommendations for preferred load cases in adhesive bonds [35], where shear is preferred to normal loads. That also has to do with the fact that perfect orthogonality cannot be reached in practice [35].

On a more general level, the mechanical properties of inkjet 3D printed VeroWhitePlus material found are similar to other studies: $E_t = 2.7$ to 2.8 GPa and $US_t = 41$ to 69 MPa [13, 14]. Stankovic et al. [15, 16] also investigated the Poisson's ratio and found values of $\nu = 1.17$ to 1.18 g/cm^3 . In comparison to other polymers, a strong similarity with Nylons is found, which has $E =$

1.8 to 3.5 GPa, $\sigma_y = 49$ to 87 MPa, $\sigma_{TS} = 100$ MPa and $\nu = 1.1$ to 1.2 g/cm³ [36]. This information allows to make educated guesses of unknown properties of the used material, such as shear moduli, which are important in numerical studies. It is also common in other, more traditional manufacturing processes that the resulting parts have mechanical anisotropies [37, 38]. For example, thermoplastic materials have different properties in the flow direction compared to the cross-flow direction, which is caused when the shear stresses in the flow orient the polymer chains, leading to higher strength. There are also other properties that induce anisotropy, such as injection speed, melt and mold temperature, shrinkage and wall thickness [38]. In non-optimized cases, the variations in the mechanical properties can exceed 25% [37], which makes it comparable to the inkjet 3D-printing process. An advantage of the anisotropy of AM compared injection molding, however, is that the direction of the anisotropy can often be actively controlled with less restrictions. Since the software on the printers do not have information on the load introduction and direction, other objectives are used for the optimization of the print orientation; usually the cost in terms of required support material and printing time. It is assumed, however, that in the future, software developers will include a feature to find the optimal build orientation for a given load case, for example [39].

6. Conclusions

First, for the first time, a mixture design was used to measure the effect of build orientation and, although having its roots in different areas, has proven to be an accurate and efficient tool to analyze the mechanical properties in a three-dimensional space.

Second, the findings of this study indicate that, when considering all possible build orientations, comparable properties to established processes such as injection molding can be reached in terms of anisotropy.

Third, the anisotropy in inkjet 3D printed parts has been investigated on a state-of-the-art printer to a high level of accuracy. The findings will inform designers, enable better predictions and create stronger parts by taking into account the dominating effects of shear stresses when the load directions are not aligned parallel to the main axes.

Acknowledgements

The research is supported by the ETH Zurich, Seed Project SP-MaP 02-14, "Additive Manufacturing of Complex-Shaped Parts with Locally Tunable Materials".

References

- [1] P. Kulkarni, A. Marsan, D. Dutta, A review of process planning techniques in layered manufacturing, *Rapid Prototyping Journal* 6 (2000) 18–35.
- [2] R. Hague, S. Mansour, N. Saleh, Material and design considerations for rapid manufacturing, *International Journal of Production Research* 42 (2004) 4691–4708.
- [3] P. Alexander, S. Allen, D. Dutta, Part orientation and build cost determination in layered manufacturing, *Computer- Aided Design* 30 (1998) 343–356.
- [4] D. Frank, G. Fadel, Expert system-based selection of the preferred direction of build for rapid prototyping processes, *Journal of Intelligent Manufacturing* 6 (1995) 339–345.
- [5] Y. Zhang, A. Bernard, R. Harik, K. Karunakaran, Build orientation optimization for multi-part production in additive manufacturing, *Journal of Intelligent Manufacturing* (2015) 1–15.

- [6] H.-S. Byun, K. H. Lee, Determination of the optimal build direction for different rapid prototyping processes using multi-criterion decision making, *Robotics and Computer-Integrated Manufacturing* 22 (2006) 69–80.
- [7] M. Taufik, P. K. Jain, Role of build orientation in layered manufacturing: a review, *International Journal of Manufacturing Technology and Management* 27 (2013) 47–73.
- [8] S.-H. Ahn, M. Montero, D. Odell, S. Roundy, P. K. Wright, Anisotropic material properties of fused deposition modeling abs, *Rapid Prototyping Journal* 8 (2002) 248–257.
- [9] K. Chin Ang, K. Fai Leong, C. Kai Chua, M. Chandrasekaran, Investigation of the mechanical properties and porosity relationships in fused deposition modelling-fabricated porous structures, *Rapid Prototyping Journal* 12 (2006) 100–105.
- [10] A. K. Sood, R. Ohdar, S. Mahapatra, Parametric appraisal of mechanical property of fused deposition modelling processed parts, *Materials & Design* 31 (2010) 287–295.
- [11] M. Barclift, C. Williams, Examining variability in the mechanical properties of parts manufactured via polyjet direct 3d printing, *International Solid Freeform Fabrication Symposium*, Austin, TX (2012).
- [12] C. W. J.P. Moore, Fatigue characterization of 3d printed elastomer material, *International Solid Freeform Fabrication Symposium*, Austin, TX (2012).
- [13] J. Mueller, S. Kim, K. Shea, C. Daraio, Tensile properties of inkjet 3d-printed parts: Critical process parameters and how to efficiently analyze them, *ASME Computers and Information in Engineering Conference*, Boston, MA (2015).
- [14] J. Mueller, K. Shea, C. Daraio, Mechanical properties of parts fabricated with inkjet 3d printing through efficient experimental design, *Materials & Design* 86 (2015): 902-912
- [15] T. Stankovic, J. Mueller, P. Egan, K. Shea, Optimization of additively manufactured multi-material lattice structures using generalized optimality criteria, in: *International Design Engineering Technical Conferences and Computers and Information in Engineering Conference*, ASME, 2015.
- [16] T. Stankovic, J. Mueller, P. Egan, K. Shea, A generalized optimality criteria method for optimization of additively manufactured multi-material lattice structures, *Journal of Mechanical Design*, Special issue on "Design for Additive Manufacturing" (2015).
- [17] A. F2792-12a, Standard Terminology for Additive Manufacturing Technologies, West Conshohocken, PA, 2012.
- [18] A. Kesy, J. Kotlinski, Mechanical properties of parts produced by using polymer jetting technology, *Archives of Civil and Mechanical Engineering X* (2010).
- [19] D. Blanco, P. Fernandez, A. Noriega, Nonisotropic experimental characterization of the relaxation modulus for polyjet manufactured parts, *Journal of Materials Research* 29 (2014) 1876–1882.
- [20] A. Pilipovi, P. Raos, M. Sercer, Experimental analysis of properties of materials for rapid prototyping, *The International Journal of Advanced Manufacturing Technology* 40 (2009) 105–115.
- [21] L. Vieira, R. Paggi, G. Salmoria, Thermal and dynamic-mechanical behavior of fullcure 3d printing resin postcured by different methods, in: *Innovative Developments in Virtual and Physical Prototyping: Proceedings of the 5th International Conference on Advanced Research in Virtual and Rapid Prototyping*, Leiria, Portugal, 28 September-1 October, 2011, CRC Press, 2011, p. 385.
- [22] A. Cazan, P. Morer, L. Matey, Polyjet technology for product prototyping: Tensile strength and surface roughness properties, *Proceedings of the Institution of Mechanical Engineers, Part B: Journal of Engineering Manufacture* 228 (2014) 1664–1675.
- [23] Alphacam, Kunststoffspritzformen aus dem 3d drucker, http://www.alphacam.de/dynamic/ksf/Praesentation_PolyJet_Form.pdf, 2014. Accessed: 2014-12-03.
- [24] B. Caulfield, P. McHugh, S. Lohfeld, Dependence of mechanical properties of polyamide components on build parameters in the sls process, *Journal of Materials Processing Technology* 182 (2007) 477–488.
- [25] C. C. Chen, P. A. Sullivan, Predicting total build-time and the resultant cure depth of the 3d stereolithography process, *Rapid Prototyping Journal* 2 (1996) 27–40.
- [26] J. Manguia, J. Ciurana, C. Riba, Neural-network-based model for build-time estimation in selective laser sintering, *Proceedings of the Institution of Mechanical Engineers, Part B: Journal of Engineering Manufacture* 223 (2009) 995–1003.
- [27] J. Giannatsis, V. Dedoussis, L. Laios, A study of the build-time estimation problem for stereolithography systems, *Robotics and Computer-Integrated Manufacturing* 17 (2001) 295–304.
- [28] I. Campbell, J. Combrinck, D. de Beer, L. Barnard, Stereolithography build time estimation based on volumetric calculations, *Rapid Prototyping Journal* 14 (2008) 271–279.
- [29] G. P. Kumar, S. P. Regalla, Optimization of support material and build time in fused deposition modeling (fdm), *Applied Mechanics and Materials* 110 (2012) 2245–2251.
- [30] G. A. Teitelbaum, Proposed build guidelines for use in fused deposition modeling to reduce build time and material volume, ProQuest, 2009.
- [31] J. A. Cornell, Experiments with mixtures: designs, models, and the analysis of mixture data, vol.895, John Wiley & Sons, 2011.
- [32] A. D695-10, Standard Test Method for Compressive Properties of Rigid Plastics, West Conshohocken, PA, 2010.
- [33] A. D638-10, Standard Test Method for Tensile Properties of Plastics, West Conshohocken, PA, 2010.
- [34] G. Z. Voyiadjis, P. I. Kattan, *Mechanics of composite materials with Matlab*, Springer Science & Business Media, 2005.
- [35] A. J. Kinloch, *Adhesion and adhesives: science and technology*, Springer Science & Business Media, 1987.
- [36] M. Ashby, D. Jones, *Engineering Materials 1: An Introduction to Properties, Applications and Design*, Butterworth-Heinemann, 2012.
- [37] M. Fujiyama, H. Awaya, S. Kimura, Mechanical anisotropy in injection-molded polypropylene, *Journal of Applied Polymer Science* 21 (1977) 3291–3309.
- [38] F. Johannaber, W. Michaeli, *Handbuch Spritzgießen*, Hanser, 2002.
- [39] A. Rinaldi, Optimization of object printing orientation, Semester thesis, ETH Zurich, Switzerland, 2015.